Electrochimica Acta 135 (2014) 301–310

Contents lists available at ScienceDirect

Electrochimica Acta

journal homepage: www.elsevier.com/locate/electacta

Spectroscopic and electrochemical studies of high-valent water soluble manganese porphyrine. Electrocatalytic water oxidation

Maria Alejandra Luna, Fernando Moyano, Leonides Sereno, Fabiana D'Eramo *

Departamento de Química. Facultad de Ciencias Exactas, Físico-Químicas y Naturales. Universidad Nacional de Río Cuarto. Agencia Postal Nº 3 - 5800- Río Cuarto, Córdoba, Argentina

ARTICLE INFO

Article history:
Received 11 January 2014
Received in revised form 22 April 2014
Accepted 27 April 2014
Available online 4 May 2014

Keywords:
Manganese porphyrin
Electrocatalysis
Electrochemistry
Water oxidation

ABSTRACT

We report herein the catalytic oxidation of water to molecular oxygen with water-soluble 5,10,15,20-tetra(N-methylpyridyl) porphyrinato manganese (III) chloride, $[PMn(III)]Cl_5$. The homogeneous chemical and electrochemical oxidation of $[PMn(III)]Cl_5$ was studied in aqueous buffer solution by UV-vis and cyclic voltammetry techniques. Firstly, $[PMn(III)]Cl_5$ was characterized by spectroscopy in pH 7 and 10, measuring the changes produced by oxidation with a chemical agent. These studies showed that intermediates with higher oxidation states, $[PMn(IV)=O]Cl_4$ and $[PMn(V)=O]Cl_5$, are formed under these conditions and they are more stable at pH 10 at room temperature. The same result was obtained by electrochemical oxidation.

The electrochemical studies showed that $[PMn(III)]Cl_5$ is adsorbed on glassy carbon electrode surface. However, this does not help explain the high oxidation current obtained in both pHs at high anodic potentials. We demonstrated that these currents, in the cyclic voltammperogram of the $[PMn(III)]Cl_5$, are due mainly to the water catalytic oxidation by the $[PMn(V)=O]^{+5}$ intermediate. Besides, we show that chloride ion present in the porphyrin structure can also be oxidized by the same mechanism.

1. Introduction

Porphyrins are central to the energy-transforming systems of biology: photosynthesis and respiration. Their function in these systems is based on their versatile redox properties.

In particular, synthetic manganese porphyrins derived from Mn(III)*meso*tetraphenylporphyrin, (TPP)Mn(III) show the catalytic ability to mimetize various biological systems in homogenous or heterogeneous catalysis [1–3]. Furthermore, these macromolecules have been employed as catalysts in a variety of oxidation reactions [4], including olefin epoxidation [1,5–8], hydroxylation of alkenes and alkanes [9–11] and oxidative degradation of pollutants and hazardous waste [12,13], and usually show similar or better catalytic properties than their iron analogs. An integral part of the research in these fields has been the isolation of the high-valent metalloporphyrin intermediates involved in these processes.

Evidence of the existence of high-valent Mn-porphyrin intermediates was provided when Willner et al. [14] reported the preparation of porphyrin-manganese(IV)-oxo intermediate, (porph)Mn(IV)=O, from the reaction of (TPP)Mn(III) and iodosobenzene. In this case, the manganese atom is in its oxidized state (IV) where the counterion that occupied the axial position of the porphyrin ring was replaced by an oxygen atom; being this the only change in the molecule structure. Subsequently, Groves et al. [15–17] reported the first detection of a reactive porphyrin-manganese(V)-oxo intermediate, (porph)Mn(V)=O in aqueous and non-aqueous media. This species, however, is not stable and rapidly converts to (porph)Mn(IV)=O intermediate and it is then reduced slowly to (porph)Mn(III) in neutral medium. The porphyrin ring is doubly deprotonated, with the result that (porph)Mn(III) and (porph)Mn(V)=O are cationic, whereas (porph)Mn(IV)=O species are neutral [18].

Review of the literature shows that there is relatively little research on the electrochemical generation "in situ" of the high-valent metalloporphyrin intermediates [5,19,20], compared with that using chemical reagents [5,13]. Also, the studies have focused mostly on non-aqueous systems.

However, the following advantages can be listed in favor of the use of electrochemical methods: i) the electrode can act as an oxidant or reductant to generate an active species from the transition metal complex resulting in a clean reaction mixture and, ii) the reaction rate and selectivity can be manipulated by varying the electrode potential and/or the choice of electrocatalyst.

* Corresponding author. Tel.: +54 358 4676233; fax: +54 358 4676233.
E-mail addresses: lsereno@exa.unrc.edu.ar (L. Sereno), fderamo@exa.unrc.edu.ar (F. D'Eramo).

http://dx.doi.org/10.1016/j.electacta.2014.04.157
0013-4686/

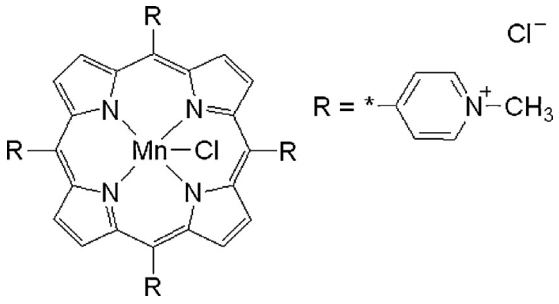

Scheme 1. Chemical structure of [PMn(III)]Cl_5.

During the past several years there has been a number of electrochemical studies both aqueous and nonaqueous media. In both media, (porph)Mn(III) may be electrochemically reduced in a single electron transfer step to yield a porphyrin containing a Mn(II) central ion, then the anion radical and dianion of (porph)Mn(II) may be formed [21]. Moreover, the (porph)Mn(III) complex may also be oxidized at the macrocycle or the metal center, giving either (porph)Mn(III) cation radicals and dications or (porph)Mn(IV) = O and $[(porph)Mn(V)=O]^+$ intermediate, depending upon the solvent, counterion on (porph)Mn(III), pK, and/or steric effects of any bound ligands as well as the porphyrin ring basicity [13,22,23].

Czernuszewicz et al. [24] reported the first identification of (porph)Mn(IV) = O bond, formed by electrochemical oxidation of (porph)Mn(III) in hydroxide media, using resonance Raman and infrared spectroscopy. Later, Chen et al. [20] reported the first $[(porph)Mn(V)=O]^+$ intermediate generated electrochemically in aqueous basic solution at room temperature and it was characterized by spectroelectrochemical methods. However, the authors have not investigated extensively the redox mechanism of porphyrin under these conditions especially at high anodic potentials.

The main objective of this work was to elucidate the manganese porphyrins electrooxidation mechanism in aqueous media and then check the catalytic capacity of the intermediates formed. Water soluble 5,10,15,20-tetra(N-methylpyridyl) porphyrinato manganese (III) chloride, [PMn(III)]Cl_5, was used in this study. In this work the intermediate species observed during the oxidative chemical reaction and the electrochemical oxidation of [PMn(III)]Cl_5 were studied by UV-Vis and cyclic voltammetry techniques, respectively. The results described here indicate that both, the chloride ion present in the porphyrin structure and the water of the reaction medium, are the active species that could be responsible for the observed catalytic current at high potentials.

2. Experimental

All reagents and solvents were of analytical grade and used without further purification. The metallopophyrin 5,10,15,20-tetra(N-methylpyridyl) porphyrinato manganese (III) chloride, [PMn(III)]Cl_5, was obtained from Aldrich. Its chemical structure is shown in Scheme 1.

Stock solutions of [PMn(III)]Cl_5 were prepared by dissolving the appropriate [PMn(III)]Cl_5 amount in water. Working solutions were prepared by accurate serial dilution from the stock solutions of [PMn(III)]Cl_5 using phosphate buffer solution of pH 7 or 10. The solutions of [PMn(III)]Cl_5, at pH 7 and 10, obey the Lambert-Beer law (λ = 462 nm, $\log(\varepsilon/l\,mol^{-1}cm^{-1})$ = 5.12 and 5.04, respectively). Thus, there is no evidence of any kind of aggregation in aqueous solution. This property was used to determine the concentration of the working solutions.

Phosphate buffer solutions (pK_{a1} = 2.23, pK_{a2} = 7.21 and pK_{a3} = 12.32) [25] were employed as a supporting electrolyte. In this work, only phosphate buffer solutions of pH 7 and 10 were using. The pH 7 phosphate buffer solutions were prepared by mixing 0.7 mol dm^{-3} NaH_2PO_4 dehydrates (Fluka) and the pH was adjusted to 7 by addition of NaOH solution (ionic strength, 1.23). The pH 10 phosphate buffer solutions were prepared using 0.4 mol dm^{-3} Na_2HPO_4 (ionic strength, 1.19). This phosphate buffer solution was used in all experiments except when otherwise indicated.

The oxidant solutions were prepared by dissolving the appropriate "oxone", amount in water. "Oxone", a stable water soluble oxidant with approximate composition $2KHSO_5.KHSO_4.K_2SO_4$, is widely used for the oxidation of various organic molecules and is also an efficient single oxygen atom donor in metal porphyrin complex catalyzed reactions [26,27].

All solutions were prepared with ultrapure water from LABCONCO equipment model 90901-01 (HPLC grade water). The solutions were thoroughly degassed by bubbling high purity nitrogen priori to electrochemical experiments. Contact with atmospheric CO_2 was minimized by maintaining nitrogen over solutions during the electrochemical experiments. The working temperature was kept constant at 20 ± 0.1 C for all measurements using a LAUDA K4R thermostat-cryostat. The pH was adjusted by using digital pH-meter (Orion 8104 Ross (pH 0–14) combination electrode).

The UV-visible spectra were obtained with a Hewlett-Packard 8452A spectrophotometer with diode array.

Electrochemical measurements were carried out using an AUTOLAB PGSTAT 30 potentiostat/galvanostat, run with GPES software, version 4.9 (Eco Chemie, Utrech, The Netherlands). A conventional three-compartment cell was used with a glassy carbon electrode (GC) disk (BAS, = 3 mm, A = 0.071 cm^2) as the working electrode, a Pt foil as the auxiliary electrode and an aqueous potassium saturated calomel electrode (SCE) as the reference electrode. A positive feedback technique was used to compensate the IR drop. The working electrode was polished with 0.3 μm alumina slurry, rinsed with a copious amount of triply distilled water and then sonicated for 5 min to remove any residual polishing material. Then, the GC electrode was activated electrochemically in 1 mol dm^{-3} NaOH aqueous solution by applying a potential step from 0 to +1.2 V over 5 min according to the procedure previously described by Anjo et al. [28].

Potentiometric titrations were carried out using a cell with a silver wire as indicator electrode and a SCE as the reference electrode. The solution employed in these experiments was a 1×10^{-3} mol dm^{-3} [PMn(III)]Cl_5 which was titrated with 0.034 mol dm^{-3} $AgClO_4$ solution. The method was verified by using a 8.2×10^{-3} mol dm^{-3} NaCl solution.

Caution! Perchlorate salts of metal complexes are potentially explosive and should be handled with care.

3. Results and Discussion

3.1. Spectral characterization of high–oxidation state [PMn(IV) = O]Cl_4 and [PMn(V) = O]Cl_5 intermediates

The chemical oxidation of 5×10^{-6} mol dm^{-3} [PMn(III)]Cl_5 in presence of stoichiometric amount of "oxone" in pH 7 phosphate buffer solutions was analyzed by UV-vis spectrophotometry. The spectrophotometer was programmed to acquire a UV-vis spectrum every 10 s. Fig. 1A shows the spectra of the [PMn(III)]Cl_5 at the beginning of the experiment which is characterized by an intense Soret band at 462 nm (solid line)) and when stoichiometric amount of "oxone" was added (dash line). As can be seen, addition of "oxone" to the reaction solution containing porphyrin caused immediate generation of a new species, [PMn(IV) = O]Cl_4, with a strong blue-shifted Soret band at 428 nm and with isosbestic points at 387 and 448 nm. Kinetic profiles were obtained

Table 1
Molar extinction coefficient for [PMn(III)]Cl_5 and intermediates [PMn(IV)]Cl_4 [PMn(IV)=O]Cl_4 and [PMn(V)]Cl_5 [PMn(V)=O]Cl_5 under the indicated pH conditions.

	pH 7		pH 10		
λnm	ε [PMn(III)]Cl_5 $(mol/dm^3)^{-1}cm^{-1}$	ε [PMn(IV)]Cl_4 [PMn(IV)=O]Cl_4 $(mol/dm^3)^{-1}cm^{-1}$	ε [PMn(III)]Cl_5 $(mol/dm^3)^{-1}cm^{-1}$	ε [PMn(IV)]Cl_4 [PMn(IV)=O]Cl_4 $(mol/dm^3)^{-1}cm^{-1}$	ε [PMn(V)]Cl_5 [PMn(V)=O]Cl_5 $(mol/dm^3)^{-1}cm^{-1}$
462	131969	26414	111025	23415	31438
428	30189	93703	24052	82023	83986
443	------	------	27462	52277	104234

by monitoring the time-dependent absorbance changes at 462 and 428 nm (Fig. 1A inset). The molar extinction coefficients for [PMn(III)]Cl_5, and [PMn(IV) = O]Cl_4 species were obtained from corresponding absorption spectra (Table 1) and the concentration calculated by matrix methods [29]. As can be seen, the intermediate [PMn(IV) = O]Cl_4, monitored at 428 nm, spontaneously decays accompanied by concurrent recovery of [PMn(III)]Cl_5 monitored at 462 nm after about half an hour. These observations are consistent with those of Groves on the same system [17]. However, we have found that conventional UV-vis spectrophotometry technique could not be able to detect [PMn(V) = O]Cl_5 specie since it is unstable under these conditions.

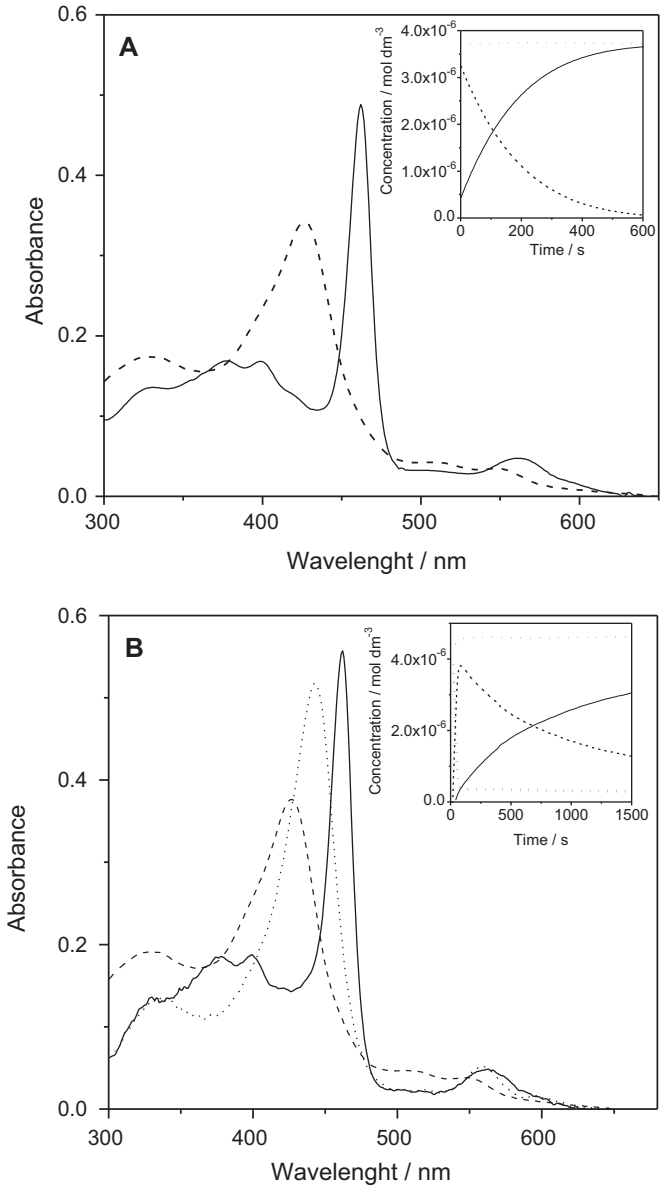

Fig. 1. Electronic absorption spectra for the stoichiometric reaction of oxono and: **A)** 3.7×10^{-6} mol dm^{-3} [PMn(III)]Cl_5 in pH 7 phosphate buffer solution, **B)** 5×10^{-6} mol dm^{-3} [PMn(III)]Cl_5 in pH 10 phosphate buffer solution. (—) [PMn(III)]Cl_5 electronic absorption spectra, (- - -) [PMn(IV) = O]Cl_4 electronic absorption spectra and (···) [PMn(V) = O]Cl_5 electronic absorption spectra. Inset A: kinetic profiles for (—) [PMn(III)]Cl_5 monitored at 462 nm, (- - -) [PMn(IV) = O]Cl_4 monitored at 428 nm, (···) [PMn(V) = O]Cl_5 monitored at 443 nm and (●●●) mass balance, from the same data set Fig. 1A. Inset B: idem as in Inset A for pH 10 phosphate buffer solution.

Thus, the experiment was repeated using different solution pHs. The most interesting results were obtained in pH 10 phosphate buffer solutions (Fig. 1B). In these cases, the reaction of [PMn(III)]Cl_5 with stoichiometric amount of "oxone" led to the formation of a new intermediate, [PMn(V) = O]Cl_5, with a strong Soret maximum at 443 nm (dotted line). Then, the intermediate [PMn(V) = O]Cl_5 decayed to [PMn(IV) = O]Cl_4 (dash line). These results are consistent with those reported by other authors [17,20]. Kinetic analysis of the data indicates that the [PMn(IV) = O]Cl_4 intermediate can be totally reversed to its tri-valent form after about 20 h (Fig. 1B inset), which shows that it is notably more stable at pH 10 than at pH 7.

In conclusion, these results suggest that there are some species in the solution that act as reducing agent to convert the intermediate [PMn(V) = O]Cl_5 to [PMn(IV) = O]Cl_4 and it to [PMn(III)]Cl_5. We propose that there are two competing species: the chloride ion present in porphyrine structure and water of the reaction media (see below).

3.2. Electrochemistry of [PMn(III)]Cl_5

The cyclic voltammograms of the [PMn(III)]Cl_5 in pH 7 phosphate buffer solutions are shown in Fig. 2A and compared with the corresponding voltammograms obtained at pH 10 (Fig. 2B). As can be seen, [PMn(III)]Cl_5 exhibited a well-defined quasi-reversible redox couple in the potential range from 0.0 to -0.4 V (peak I) which can be assigned to the porphyrin Mn(III/II) couple. This agrees with the result obtained in other manganese porphyrins in non aqueous media [30] and more recently in aqueous media [20,21]. The redox potential of this couple is pH dependent and shifts to less negative values in pH 10 solutions. Furthermore, the cyclic voltammogram for the oxidation of [PMn(III)]Cl_5 in the range potential 0.0 to 1.0 V exhibits a quasi-reversible redox couples (peak II) that correspond to metal oxidation forming [PMn(IV) = O]Cl_4 species [20,31]. A significant shift in redox potential towards more negative values coupled with an increase in the reversibility was observed when pH is raised from 7 to 10. This confirms the result obtained by conventional UV-vis spectrophotometric technique that the [PMn(IV) = O]Cl_4 intermediate is notably more stable at alkaline pH.

In addition, when the anodic potential was increased above 1.0 V (Fig. 3 A and B), a wave appeared at a higher potential (peak III) but the corresponding cathodic wave was not observed upon reversal scan at both pHs. The main characteristic of this peak is the high value current compared with the peaks I and II. The peak III includes further oxidation of [PMn(IV) = O]Cl_4 intermediate to [PMn(V) = O]Cl_5 intermediate [17,20] although, it may be followed by further oxidation at the porphyrin ring to form different oxidized species, which are known to be unstable in aqueous solution, as suggested by Trofimova et al. [31]. However, the authors were

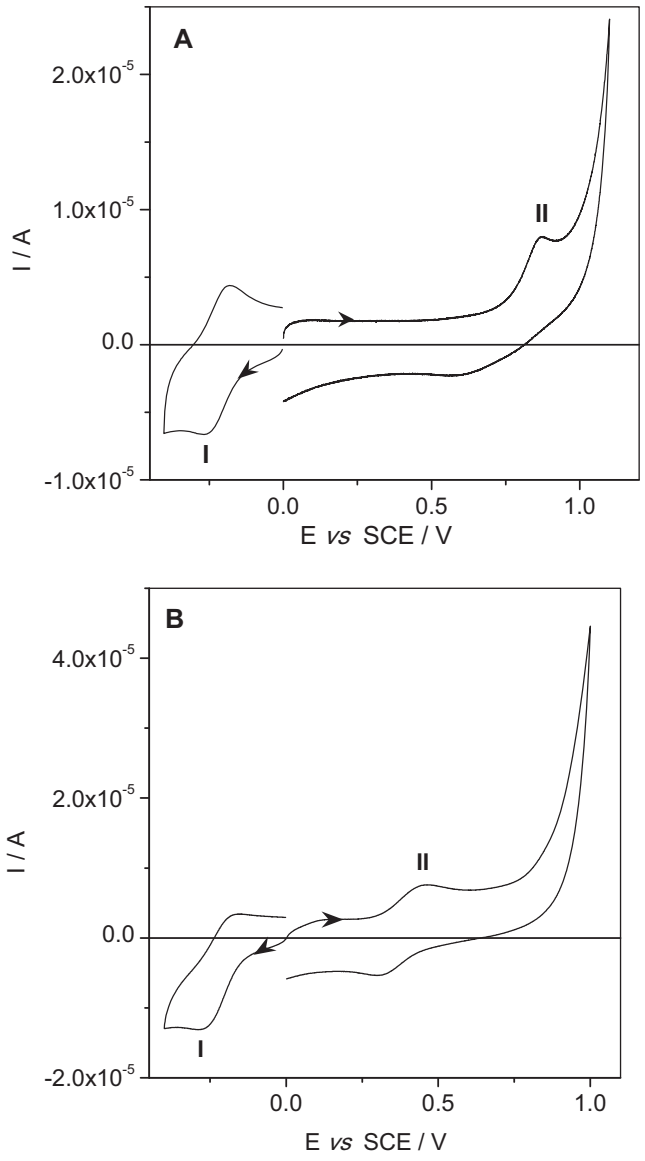

Fig. 2. Cyclic voltammogram of 5×10^{-4} mol dm^{-3} [PMn(III)]Cl_5 at 0.10 Vs^{-1}, potential range from 0.0 to -0.4 V and 0.0 to 1.0 V **A)** in pH 7 phosphate buffer solution, **B)** in pH 10 phosphate buffer solution. The arrows indicate the direction of potential sweep.

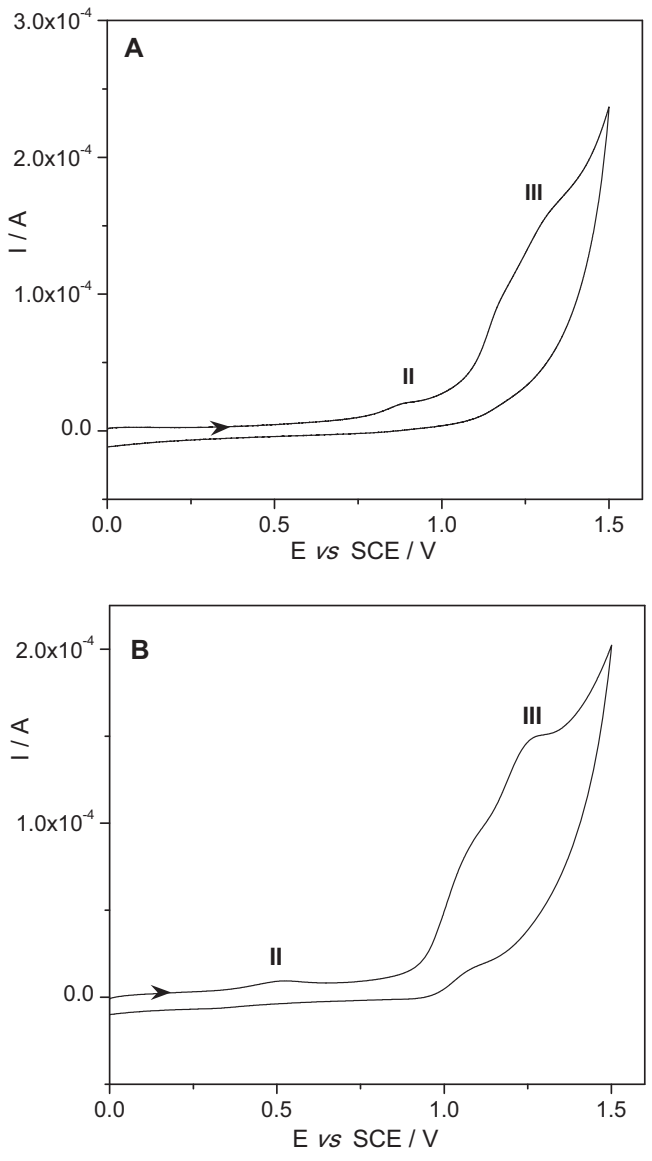

Fig. 3. Cyclic voltammogram of 5×10^{-4} mol dm^{-3} [PMn(III)]Cl_5 at 0.10 Vs^{-1}, potential range from 0.0 to 1.5 V **A)** in pH 7 phosphate buffer solution, **B)** in pH 10 phosphate buffer solution.

unable to discriminate between these two processes. We consider that only metal oxidation occurs at these potentials and the high peak III current is due to electrocatalytic reaction of [PMn(V) = O]Cl_5 (see below).

As can be seen in Fig. 3, the peak III potential also shifts toward less positive values with increased pH.

Therefore, due to the natural complexity of the peaks I, II and III we perform an in-depth investigation of each both pHs.

3.2.1. *Preliminary studies on peaks I, II and III*

3.2.1.1. Adsorption of [PMn(III)]Cl_5 on GC electrode. An exhaustive study of the peaks I, II and III, in both pHs, shows that the peak currents are higher than predicted by the Randles - Sevcik equation (1) for a reversible, diffusion controlled process that involves the transfer of one-electron [32] (see Figs. 2 and 3):

$$Ip = 0.4463nFAC_O D_O^{1/2} \left(\frac{nF}{RT}\right)^{1/2} v^{1/2} \quad (1)$$

where n represents the number of electrons transferred (assume equal to 1), T the absolute temperature of the system (293 K), $D_O = 1.2 \times 10^{-6}$ cm^2 s^{-1} (reported in the literature [33,34]), $C_O = 5 \times 10^{-7}$ mol cm^{-3}, A = 0.071 cm^2, v = 0.1 V s^{-1} and the other parameters have their usual meaning. Theoretical current value is: 3.3×10^{-6} A. It was found that the average experimental current values for the peak I, II and III were higher than theoretical value in both pHs (Table 2).

Moreover, it should be noticed that the diffusion coefficient of the redox processes for peak I, II and III is the same; thus the current

Table 2
Peak current values (I_p) of 5×10^{-4} mol dm^{-3} [PMn(III)]Cl_5 in phosphate buffer solutions at 0.10 Vs^{-1}. Theoretical I_p value for diffusion controlled process that involves one-electron transfer: 3.3×10^{-6} A.

pH	I_{pI}/A	I_{pII}/A	I_{pIII}/A
7	5.2×10^{-6}	6.2×10^{-6}	1.2×10^{-4}
10	10×10^{-6}	5.3×10^{-6}	1.4×10^{-4}

values should be similar. The global processes from the viewpoint of the charge transfer can be described by the following equations:

peakI $$[PMn(III)]^{+5} + e^- \rightleftarrows [PMn(II)]^{+4} \quad (2)$$

peakII $$[PMn(III)]^{+5} + H_2O \rightleftarrows [PMn(IV) = O]^{+4} + 2H^+ + e^- \quad (3)$$

peakIII $$[PMn(IV) = O]^{+4} \rightleftarrows [PMn(V) = O]^{+5} + e^- \quad (4)$$

Therefore, we studied if this behaviour can be attributed to adsorption process of $[PMn(III)]Cl_5$ on GC electrode surface. A similar behaviour has been reported for other metalloporphyrines [35–37].

3.2.1.1.1. Detection of $[PMn(III)]Cl_5$ adsorption in peak I. Fig. 4A (solid line) shows the cyclic voltammogram of $[PMn(III)]Cl_5$ in a 33% ACN–67% pH 7 phosphate buffer solutions mixture. Under these conditions the cyclic voltammogram shows a reversible behaviour and the resulting peak I current is controlled by diffusion in the range of sweep rate used (Fig. 4B) [32].

However, when this same analysis was performed in pH 7 phosphate buffer solutions significant changes of the shape and current densities in the voltammogram were observed (Fig. 4A (dotted line)). Results show that the cathodic peak current is larger than the anodic peak current. This asymmetric voltammogram shape is typical of a weakly adsorbed reagent on the surface of electrode [38]. More insight is obtained if we calculate the ratio between the experimental peak I current with respect to the theoretical value given by equation (1) (Fig. 4C).

Additional experiments were carried out by immersion of the GC fresh electrode in 1×10^{-3} mol dm^{-3} $[PMn(III)]Cl_5$ solution for twenty minutes at open circuit potential to ensure maximum surface coverage. Then, the electrode was rinsed with buffer solution to remove the excess $[PMn(III)]Cl_5$ and was transferred to another cell containing porphyrine-free solution. The cyclic voltammogram obtained in the cathodic sweep shows an increment of the negative current with respect to the blank current, although the peak I was not clearly defined. The intensity of cathodic current obtained from forward sweep decreases gradually with the successive scans, which indicated weak adsorption of this reagent on the electrode surface.

Similar results were also observed in pH 10 phosphate buffer solutions.

3.2.1.1.2. Detection of $[PMn(III)]Cl_5$ adsorption in peak II. The GC fresh electrode was immersed again in 1×10^{-3} mol dm^{-3} $[PMn(III)]Cl_5$ solution for twenty minutes at open circuit potential to ensure maximum surface coverage. Then, the electrode was rinsed with buffer solution to remove the excess $[PMn(III)]Cl_5$ and was transferred to another cell containing porphyrine-free solution. Fig. 5 shows the electrode response in pH 10 buffer solution, in the potential range of peak II. In this case, a well-defined peak II (after subtraction of the blank) was observed. The shape of the cyclic voltammogram is typical of confined species on the electrode surface.

Moreover, the voltammogram of $[PMn(III)]Cl_5$ is highly asymmetric suggesting a complex redox behaviour. Anodic and cathodic peaks have a width at half-height maximum of 0.252 V. This value is greater than 0.091 V at 25 °C, value expected for a thin layer cell with Nernstian behaviour for one electron for the electronic transfer [32]. It is due to repulsive interactions between molecules adsorbed on the electrode surface [39,40]. The charge for the anodic peak was 2.3×10^{-6} C from which we obtained the surface excess with a value of $\Gamma = 3.4 \times 10^{-10}$ moles cm^{-2}. The value found for Γ is similar to that obtained by Van Galen y col. [41], for a cobalto

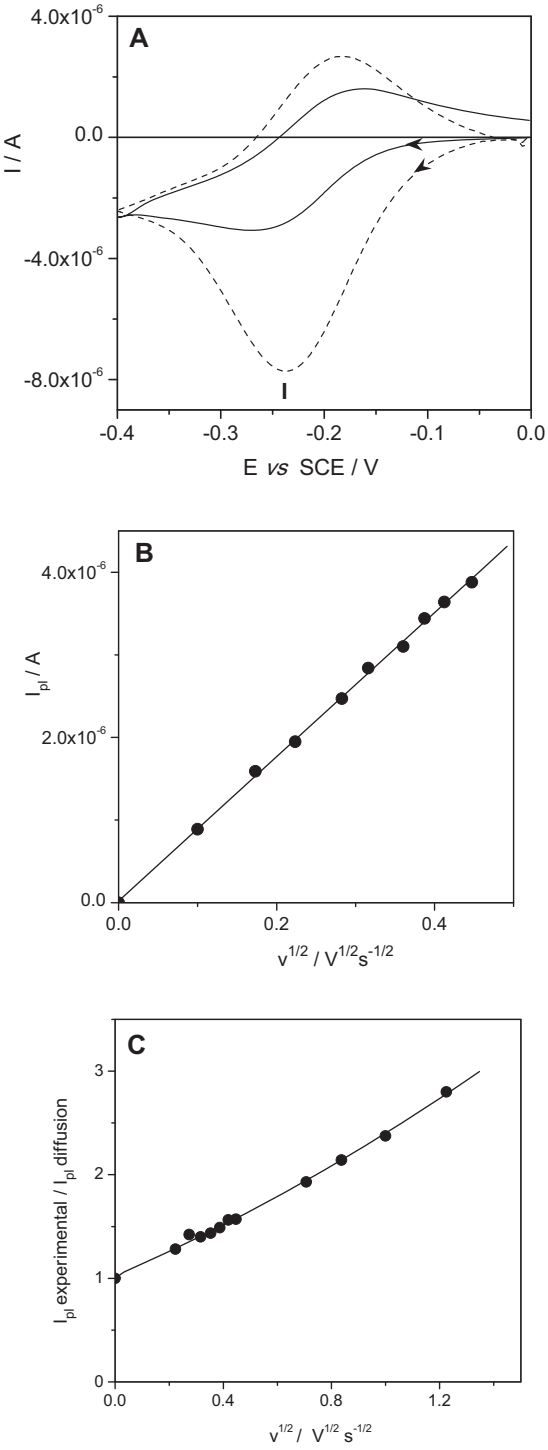

Fig. 4. A) Cyclic voltammogram of 5×10^{-4} mol dm^{-3} $[PMn(III)]Cl_5$ at 0.10 Vs^{-1} in: (—) 33% ACN - 67% pH 7 phosphate buffer solution, (- - -) pH 7 phosphate buffer solution. **B)** Correlation of the peak I current with square root of the scan rate of 5×10^{-4} mol dm^{-3} $[PMn(III)]Cl_5$ in 33% ACN - 67% pH 7 phosphate buffer solution. **C)** Ratio peak I current experimental/peak I current diffusion with square root of the scan rate of 4.2×10^{-4} mol dm^{-3} $[PMn(III)]Cl_5$ in pH 7 phosphate buffer solution.

(II) porphyrin adsorbed on polycrystalline gold electrode surface ($\Gamma = 3.3 \times 10^{-10}$ moles cm^{-2}) and it corresponds to a monolayer coverage. These results indicate that the porphyrin is adsorbed with a perpendicular orientation of the pophyrin ring with respect to the electrode plane (the area occupied by a molecule of the metalloporphyrin is 50 Å^2 [41]), which would explain the maximum packing and repulsion between porphyrin molecules.

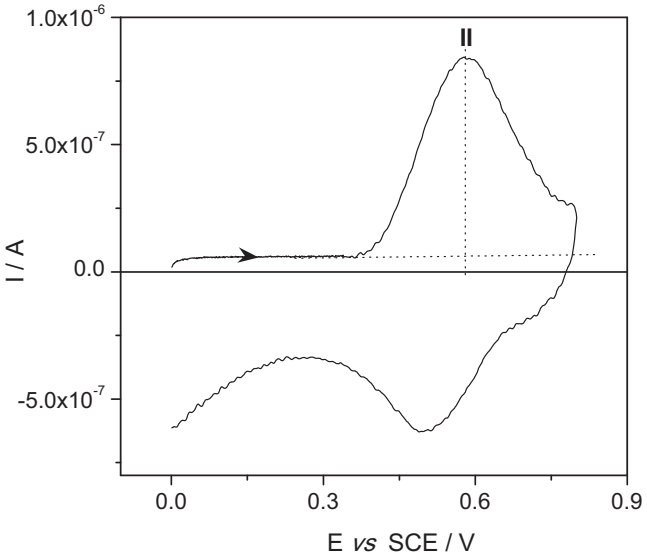

Fig. 5. Cyclic voltammogram of $[PMn(III)]Cl_5$ at 0.10 Vs^{-1} in pH 10 phosphate buffer solution after adsorption in 1×10^{-3} mol dm^{-3} $[PMn(III)]Cl_5$ solution, adsorption time: 20 min.

On the other hand, successive cycles of potential sweeps show that the peak II current decreases cycle by cycle, which would indicate that the adsorption of the reagent is weak. Also, the cathodic peak charge was 30% lower than the anodic peak charge and this shows that desorption process takes place.

When similar studies were conducted in pH 7 phosphate buffer solutions the same behaviour was observed.

The above results explain why the current of peak I and II were higher than the diffusional current, predicted by the Randles - Sevcik (Eq. (1)) for a reversible process that involves the transfer of one-electron, for both pHs.

3.2.1.1.3. Detection of $[PMn(III)]Cl_5$ adsorption in the potential range from 1.0 V to 1.5 V.. In the potential range from 1.0 V to 1.5 V the adsorption process was evidenced by performing consecutive potential scans in $[PMn(III)]Cl_5$ pH 10 phosphate buffer solutions. Fig. 6A shows a typical result. As can be observed, when the number of potential cycles is increased, a pre-peak about 1.07 V is defined. The pre-peak current increases cycle by cycle until reaching a steady state after five or six cycles (see inset in Fig. 6A). When the electrode was rinsed with a pH 10 phosphate buffer solution and it was transferred to another electrochemical cell containing porphyrine-free solution, a cyclic voltammogram, as shows in Fig. 6B, was obtained. As can be seen, a peak at 1.07 V corresponding to the potential of the pre-peak was observed.

Taking into account the potential range where the pre-peak appears, it is expected that the oxidation of the adsorbed intermediate $[PMn(IV)=O]Cl_4$ to adsorbed intermediate $[PMn(V)=O]Cl_5$ takes place.

This can be described as:

$$[PMn(IV) = O]^{+4}{}_{ads} \rightarrow [PMn(V) = O]^{+5}{}_{ads} + e- \quad (5)$$

where, $[PMn(IV)=O]^{+4}{}_{ads}$ is the intermediate $[PMn(IV)=O]Cl_4$ adsorbed on the GC electrode surface and $[PMn(V)=O]^{+5}{}_{ads}$ is the intermediate $[PMn(V)=O]Cl_5$ adsorbed on the GC electrode surface.

The net charge of pre-peak was calculated by subtracting from the total charge the corresponding background value, assuming one electron for the electronic transfer. From the net charge the apparent surface excess value (Γ) was obtained which resulted higher than the value of monolayer (see above). Therefore, systematic studies were performed varying the $[PMn(III)]Cl_5$ concentration in the range 1×10^{-5} - 5×10^{-4} mol dm^{-3} in order to obtain more

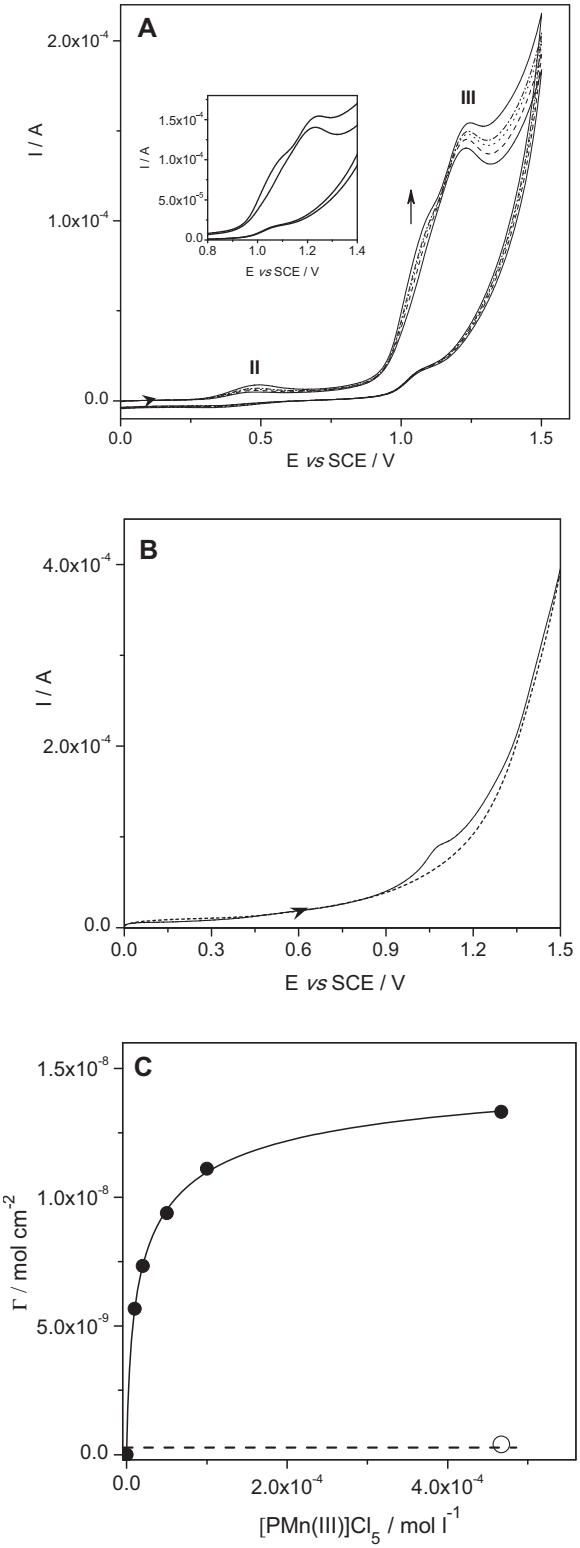

Fig. 6. A) Cyclic voltammogram of 5×10^{-4} mol dm^{-3} $[PMn(III)]Cl_5$ at 0.10 Vs^{-1} in pH 10 phosphate buffer solution. Cycle number = 6. Inset: enlargement of the zone potential between 0.8 to 1.4 V, comparing the first and the sixth cycle of potential sweep. **B)** Cyclic voltammogram of adsorbed $[PMn(V)=O]Cl_5$ at 0.10 Vs^{-1} in pH 10 phosphate buffer solution after the experiment carried out in Fig. 6A, (- - -) blank solution. **C)** Dependence of apparent surface excess with $[PMn(III)]Cl_5$ concentration, (o) surface excess value for monolayer.

information about the nature of the adsorption process. Each experiment was carried out with a fresh GC electrode surface. The electrode was placed in a cell containing a $[PMn(III)]Cl_5$ solution and submitted to successive potential sweep to reach a steady state for each $[PMn(III)]Cl_5$ concentration. Fig. 6 C shows the dependence of the Γ values on the $[PMn(III)]Cl_5$ concentration, the value for a monolayer is included for comparative purposes. These results show that the Γ were higher than the value of monolayer which is indicating that an adsorption process and a catalytic process, produced by the adsorbed intermediate $[PMn(V)=O]Cl_5$, occur. This can be described by the following equations:

$$[PMn(IV)=O]^{+4}_{ads} \longrightarrow [PMn(V)=O]^{+5}_{ads} + e- \quad (6)$$

$$[PMn(V)=O]^{+5}_{ads} + Z \xrightarrow{k_c} [PMn(IV)=O]^{+4}_{ads} + \text{product} \quad (7)$$

where Z is some species that can be oxidized by intermediate $[PMn(V)=O]Cl_{5\ ads}$ (catalysis) and k_c is an apparent catalytic constant. The k_c value along with Z and $[PMn(III)]Cl_5$ concentrations and the sweep rate determine the magnitude of charge observed for this pre-peak.

3.2.1.2. Behaviour of peak III. Taking into account the results obtained above, the intermediate $[PMn(V)=O]Cl_{5\ ads}$ produces a catalytic process at 1.07 V. However, when the anodic potential was increased above this value, the peak III could be observed. The value of the peak current (I_{pIII}) is higher than expected for a diffusion process that involves the transfer of one-electron (see Table 2).

In order to elucidate the nature of peak III experiments were carried out to demonstrate that species can be oxidized by intermediate $[PMn(V)=O]Cl_5$. As mentioned above and taking into account the redox potential of the intermediate $[PMn(V)=O]Cl_5$, we propose that the species are: chloride ion present in the porphyrin structure and the water of the reaction medium. The standard oxidation potential in aqueous media for Cl^-/Cl_2 and H_2O/O_2 couples, as a first approximation, are lower than the intermediate $[PMn(V)=O]Cl_5$ potential [25].

3.2.1.2.1. Catalytic oxidation of chloride ion by [PMn(III)]Cl₅. A set of different experiments was performed in order to test catalytic oxidation of chloride ion by $[PMn(III)]Cl_5$. The GC electrode was immersed in 5×10^{-4} mol dm^{-3} $[PMn(III)]Cl_5$ in pH 10 phosphate buffer solutions and the cyclic voltammograms were recorded. It is important to note that in this solution the chloride ions concentration is 2.5×10^{-3} mol dm^{-3} assuming that all chloride ions are electroactive. Then, different aliquots of 0.20 mol dm^{-3} NaCl stock solution were added to $[PMn(III)]Cl_5$ solution. The chloride ion concentration was increased successively to reach 0.13 mol dm^{-3}. The cyclic voltammetric responses obtained under these conditions are shown in Fig. 7A. As can be seen, the peak III current increased with the chloride ion concentration. The shape of the cyclic voltammogram did not change, this is confirmed when the cyclic voltammograms were normalized to unity. In this case, all the voltametric responses overlapped. In addition, these results indicate that GC electrode is not fouled; therefore, all experiments are comparable and depend only on the chloride ion concentration which enables a quantitative treatment of the data (see below). It is important to note that the potential range where the peak II appears was unaffected by the addition of chloride ion.

In conclusion, the peak III clearly shows an interaction between the main species involved: $[PMn(V)=O]Cl_5$ (adsorbed or at the interface electrode-solution) and chloride ion.

The same experiments were carried out in pH 10 phosphate buffer solutions free of $[PMn(III)]Cl_5$ (inset of Fig. 7A). As can be observed, in all the cases the current increases with chloride ion concentration but a characteristic peak is not observed. This behaviour is due to the fact that the chloride ion oxidation overlaps

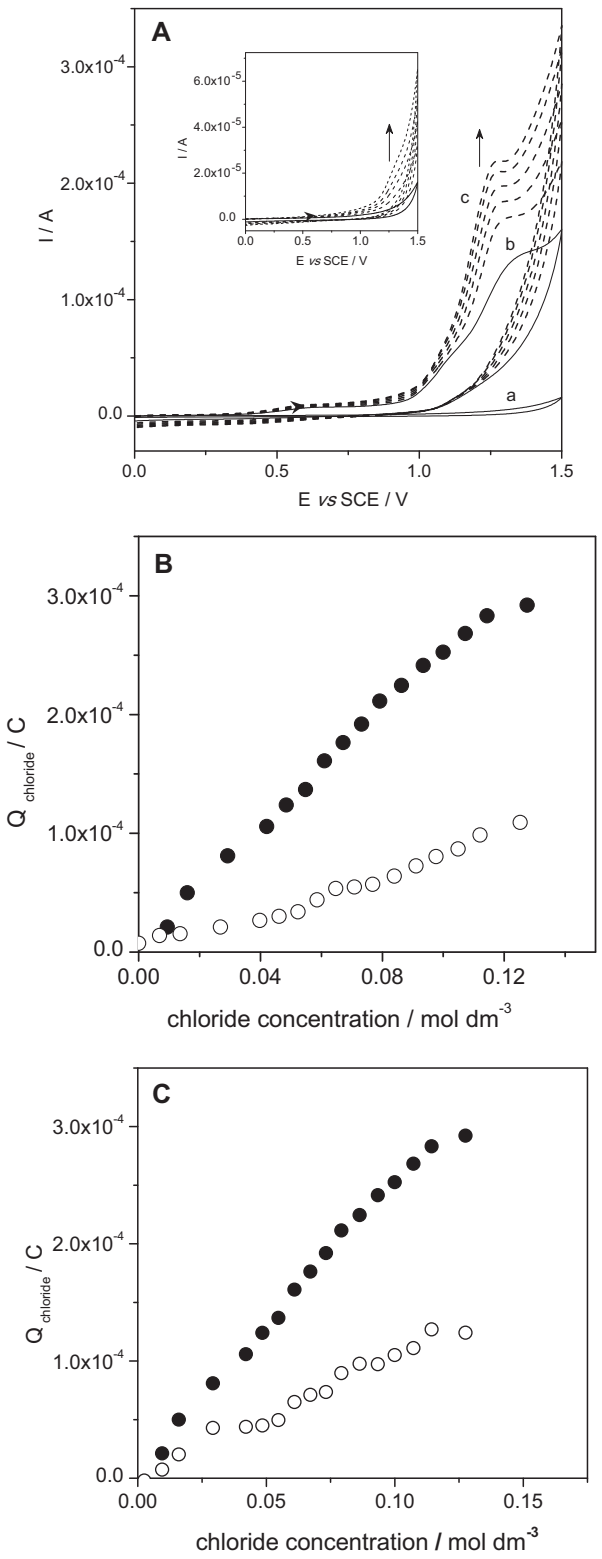

Fig. 7. A) Cyclic voltammograms of 5×10^{-4} mol dm^{-3} $[PMn(III)]Cl_5$ in pH 10 phosphate buffer solution at 0.10 Vs^{-1}, containing different chloride concentrations: (a) blank; (b) without chloride; (c) 2.9×10^{-2}; 4.5×10^{-2}; 7.3×10^{-2}; 9.3×10^{-2}; 0.13 mol dm^{-3}. Arrow indicates increased chloride concentration. Inset: Idem in pH 10 phosphate buffer solution free $[PMn(III)]Cl_5$, (solid line) blank. **B)** Oxidation charge of chloride at 0.10 Vs^{-1} at pH 10 *vs* total chloride concentration: (o) Eq. (9) and (●) Eq. (11). **C)** Effect of the pH on the chloride oxidation charge (Eq. (11)): (o) pH 7, (●) pH 10.

with water oxidation and under these conditions the oxidation of chloride ion to Cl_2 is a process with high activation overpotential.

The chloride ion electrochemical oxidation is a well known process for example in chlor-alkali cells, but in this case mixed oxide electrodes of high catalytic activity are used [42]. In conclusion, under this conditions the chloride ion is oxidized but with low yield.

Similar behaviour was also observed in pH 7 phosphate buffer solutions with or without [PMn(III)]Cl_5.

A more rigorous interpretation of these experiments requires a quantitative treatment of the data. This will show if chloride ion oxidation in the presence of [PMn(III)]Cl_5 is due to an electrocatalytic process or only the sum of independent redox processes.

For this analysis, the chloride ion oxidation charge was calculated by integration of the cyclic voltammograms in the potential range from 0.0 to 1.5 V, since the chloride ion oxidation in the absence of [PMn(III)]Cl_5 does not show characteristic peak currents. In addition, the redox process of peak II is not affected by the presence of chloride ion.

Therefore, the total charge can be represented as:

$$Q_{total} = Q_{blank} + Q_{Cl^-} \quad (8)$$

where Q_{blank} is the charge obtained by integration of cyclic voltammogram recorded in pH 10 phosphate buffer solution free of NaCl and Q_{Cl^-} is a chloride ion oxidation charge added to the solution.

Rearranging this equation, Eq. (9) is obtained:

$$Q_{Cl^-} = Q_{total} - Q_{blank} \quad (9)$$

On the other hand, when a similar analysis was carried out in [PMn(III)]Cl_5 solution, the total charge can be represented as:

$$Q_{total} = Q_{blank} + Q^o_{[PMn(III)]Cl5} + Q_{Cl^-} \quad (10)$$

where $Q^o_{[PMn(III)]Cl5}$ is a complex charge formed by diffusional and a catalytic charge (the later due to oxidation of some species of the reaction medium or to chloride ion of [PMn(III)]Cl_5). Q_{total}, Q_{blank} and Q_{Cl^-} have the same meaning as in Eq. (9). The Eq. (10) indicates that Q_{total} is a function of chloride ion concentration of the reaction medium.

Rearranging this equation, Eq. (11) is obtained:

$$Q_{Cl^-} = Q_{total} - (Q_{blank} + Q^o_{[PMn(III)]Cl5}) \quad (11)$$

where $(Q_{blank} + Q^o_{[PMn(III)]Cl5})$ is obtained by integration of voltammogram recorded in [PMn(III)]Cl_5 solution free of NaCl.

Fig. 7B shows a comparative plot of the chloride ion oxidation charge with and without [PMn(III)]Cl_5. As can be seen, the Q_{Cl^-} in presence of phorphyrine was higher than the Q_{Cl^-} in the absence of [PMn(III)]Cl_5. From this, it is concluded that intermediate [PMn(V)]Cl_5 [PMn(V)=O]Cl_5 catalyzes the chloride ion oxidation to Cl_2. However, from the experiment described above we were not able to elucidate if any other species in the solution are oxidized along with chloride ions by intermediate [PMn(V)]Cl_5 [PMn(V)=O]Cl_5 (see below). On the other hand, the same experiments were carried out at pH 7. Fig. 7C shows the results of chloride ion oxidation charge as function of chloride ion concentration at both pHs. It can be observed that the catalysis is higher at pH 10 than pH 7. This behaviour agrees with the results obtained by spectrophotometry and voltammetry, where the intermediate [PMn(IV)=O]Cl_4 and [PMn(V)=O]Cl_5 are more stable at this pH.

From these results, a method to eliminate the chloride ion from [PMn(III)]Cl_5 was carried out in order to investigate if chloride ions are the only species responsible for the high current of peak III. From now on, the studies will be carried out at pH 10.

3.2.2. Synthesis of PMn(III)X_5

$[PMn(III)]^{+5}$ chloride-free was prepared following the methodology described by Zhang et al. [18] which consists in removing chloride from [PMn(III)]Cl_5 by precipitation with $AgClO_4$ solution.

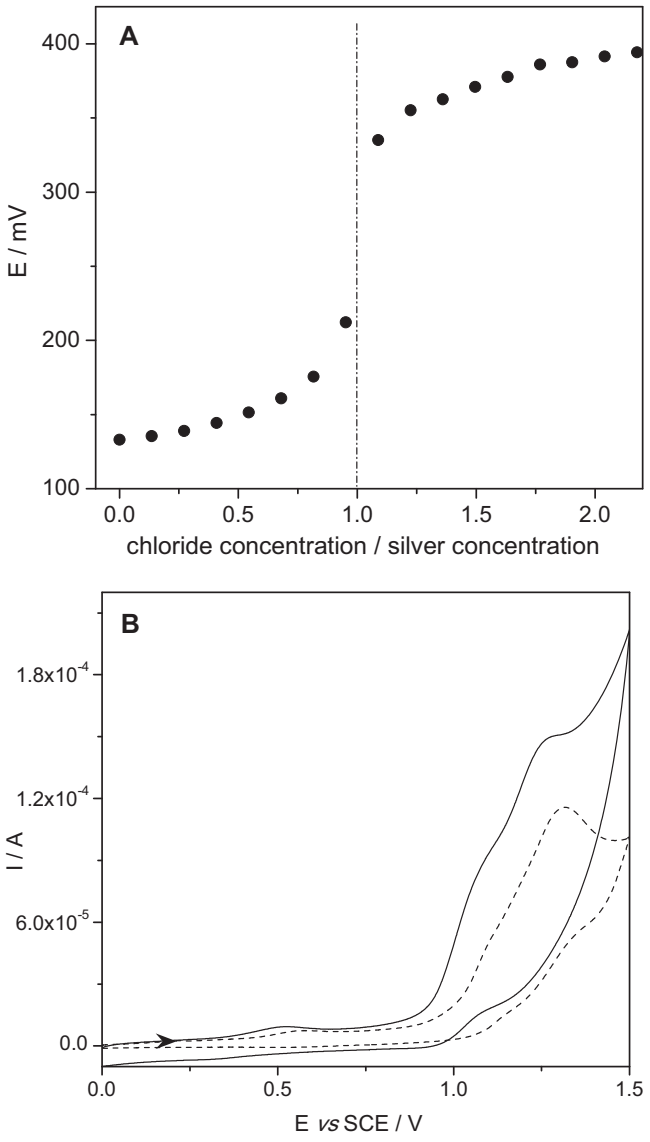

Fig. 8. **A**) Plot of E *vs* (chloride concentration/silver concentration) for potentiometric titration of 1×10^{-3} mol dm^{-3} [PMn(III)]Cl_5 with 0.034 mol dm^{-3} $AgClO_4$. **B)** Cyclic voltammograms of 5×10^{-4} mol dm^{-3}: (—) [PMn(III)]Cl_5 and (––) [PMn(III)]X_5 in pH 10 phosphate buffer solution at 0.10 Vs^{-1}.

First we investigated how many chlorides are removed from [PMn(III)]Cl_5. Thus, potentiometric titration of 1×10^{-3} mol dm^{-3} [PMn(III)]Cl_5 solution with 0.034 mol dm^{-3} $AgClO_4$ solution was performed. A typical titration curve was obtained (Fig. 8A). The experimental result indicates that five chloride ion of [PMn(III)]Cl_5 were removed.

Therefore, the synthesize of metalloprphyrine chloride-free (from now on called, PMn(III)X_5, where X is an anion present in the reaction medium, e.g. ClO_4^-, HO^-) was carried out according to the following procedure:*i)* 50 mL of a 6.0×10^{-4} mol dm^{-3} [PMn(III)]Cl_5 solution was added with solid $AgClO_4$ used in equimolar quantities. This solution was allowed to stand while protected from light and air for 24 h.*ii)* The solution was filtered through a 0.2 μm disposable filter. Then, the filtrate was added to an appropriate amount of Na_2HPO_4 in order to adjust the Na_2HPO_4 concentration to 0.4 mol dm^{-3} (it is the concentration value of pH 10 phosphate buffer solution employed for electrochemical measurements). This was performed to eliminate the silver ions that remained in solution

($K_{ps(AgCl)} = 1.8 \times 10^{-10}$, $K_{ps(Ag3PO4)} = 1.4 \times 10^{-16}$).*iii)* If of Ag_3PO_4 precipitate is formed, the solution is filtered again through a 0.2 μm disposable filter and the pH was adjusted to 10. An aliquot of this solution was placed in a glass cell for UV-vis spectrophotometer and the optical absorption spectra were registered. It is important to clarify that the [PMn(III)]X_5 UV-vis spectra look very similar to that observed for [PMn(III)]Cl_5. Aliquots of this solution were further diluted in pH 10 phosphate buffer solution to reach a concentration of 5×10^{-4} mol dm^{-3} for electrochemical studies.

In Fig. 8B the cyclic voltammogram of [PMn(III)]Cl_5 is compared to the cyclic voltammogram of [PMn(III)]X_5 under the same experimental conditions. As can be seen, the anodic charge of Mn(III)PX_5 was 40% lower than that obtained for [PMn(III)]Cl_5. However, the peak III current remains higher than the diffusional current, as was predicted by Randles -Sevcik (Eq. (1)) for a reversible process that involves the transfer of one-electron.

These results indicate that there is another species in the reaction medium that is oxidized by the intermediate [PMn(V) = O]X_5. We propose that this species is water. Although studies of Faradaic yield were not carried out for the water oxidation, we calculate a turnover number as the ratio of the peak III charge of [PMn(III)]X_5 chlorine-free respect to the theoretical charge for a reversible, diffusion controlled process that involves the transfer of one-electron ($Q_{pIII\ theoretical} = 5.8 \times 10^{-6}$ C) ($Q_{p\ III}/Q_{pIII\ theoretical}$). The approximate turnover number value obtained was 80.

The ability of the high-valent manganese porphyrine to oxidize water has been previously described by other authors using chemical and photochemical methods [43,44]. Then, Naruta et al. [45] were the first to demonstrate the catalytic oxidation of water to molecular oxygen with rigidly linked manganese porphyrin dimmers employing electrochemical methods. Despite numerous experimental and theoretical model studies, the actual mechanism for the formation of molecular oxygen is not clear and only a relatively small number of molecular water oxidation catalysts are hitherto known, with the majority of them having been discovered in the last few years. The discovery of effective and long-lived water catalysts derived from abundant and low-priced first-row transition metals remains a major objective for future research. Advances concerning this aspect might be considered indispensable in terms of a significant contribution of artificial photosynthesis applications for sustainable power generation in the near future [46].

4. Conclusions

The UV-vis spectroscopic and electrochemical studies for species generated from water soluble [PMn(III)]Cl_5 indicate that it produces high-oxidation state intermediates, [PMn(IV) = O]Cl_4 and [PMn(V) = O]Cl_5, by homogeneous chemical oxidation and electrochemical oxidation in aqueous phosphate buffer solutions of pH 7 and 10. In this work, we have shown that these intermediates are more stable at pH 10 than pH 7.

An exhaustive electrochemical study on [PMn(III)]Cl_5 revealed that the peak currents of the three peaks of porphyrin, in both pHs, were significantly higher than predicted by Randles - Sevcik (Eq. (1)) for a reversible, diffusion controlled process that involves the transfer of one-electron.

In the potential range of peaks I and II these studies have shown that [PMn(III)]Cl_5 was weakly adsorbed on the GC electrode surface. For peak II we were able to calculate the surface excess with a value of $\Gamma = 3.4 \times 10^{-10}$ moles cm^{-2} which corresponds to a monolayer coverage. The value found for Γ was similar to that obtained for others metallophorpyrines where the porphyrin adsorption occurs mainly with perpendicular orientation of the pophyrin ring with respect to the electrode plane.

On the other hand, the electrochemical behaviour of [PMn(III)]Cl_5 in the range potential 1.0 V to 1.5 V was more complex. We show that in this potential range a pre-peak was observed which corresponds to oxidation of the adsorbed intermediate [PMn(IV) = O]Cl_4 to the adsorbed intermediate [PMn(V) = O]Cl_5.

An estimate of Γ for this pre-peak showed that the obtained value was significantly higher than expected for an adsorbed monolayer value of this species.

Also, at more positive potentials of the pre-peak, a peak III was observed which shows a current significatively higher than predicted by Randles - Sevcik (Eq. (1)).

In order to explain these behaviours we propose that in addition to the adsorptive process (pre-peak, intermediate [PMn(V) = O]$^{+5}_{ads}$) a catalytic process occurs simultaneously in the interface.

Electrochemical studies show that [PMn(III)]Cl_5 catalyze oxidation of chloride ion and water to produce chlorine and oxygen at relatively low oxidation potentials.

It is worth noting that the CV electrode in combination with [PMn(III)]Cl_5 or [PMn(III)]X_5 are promising catalysts since they are effective and low cost for electrochemical generation of oxygen from water under basic conditions and this is important from the technological point of view.

Acknowledgment

The authors gratefully acknowledge financial support from Consejo Nacional de Investigaciones Científicas y Técnicas (CONICET-Argentina), Agencia Nacional de Promoción Científica y Tecnológica (ANPCYT - Argentina) and Secretaría de Ciencia y Técnica (Universidad Nacional de Río Cuarto - Argentina). M. A. Luna and F. Moyano thank CONICET for a research fellowship.

References

[1] W. Nam, Y.M. Goh, Y.J. Lee, M.H. Lim, C. Kim, Biomimetic Alkane Hydroxylations by an Iron(III) Porphyrin Complex with H_2O_2 and a High-Valent Iron(IV) Oxo Porphyrin Cation Radical Complex, Inorg. Chem. 38 (1999) 3238.
[2] X-B. Zhang, C-C. Guo, J.B. Xu, R-Q. Yu, Synthesis of acetylglycosylated metalloporphyrins and their catalysis for cyclohexane oxidation with PhIO under mild conditions, J. Mol. Catal. A: Chem. 154 (2000) 31.
[3] K.T. Moore, I.T. Horváth, M.J. Therien, Mechanistic studies of (porphinato)iron-catalyzed isobutane oxidation. Comparative studies of three classes of electron-deficient porphyrin catalysts, Inorg. Chem. 39 (2000) 3125.
[4] K-Ch. Cheung, W.-L. Wong, D.-L. Ma, T.-S. Lai, K.-Y. Wong, Transition metal complexes as electrocatalysts. Development and applications in electro-oxidation reactions, Coord. Chem. Rev. 251 (2007) 2367.
[5] B. Meunier, Metalloporphyrins as versatile catalysts for hydrocarbon oxygenations and oxidative DNA cleavage, Chem. Rev. 92 (1992) 1411.
[6] F. Vinhado, P. Martins, A. Masson, D. Abreu, E.A. Vidoto, O.R. Nascimento, Y. Lamamoto, Supported iron(III)porphyrins pentafluorophenyl-derivatives as catalysts in epoxidation reactions by H_2O_2: the role of the silica-support and sulfonatophenyl residues in the activation of the peroxidic bond, J. Mol. Catal. A: Chem. 188 (2002) 141.
[7] W. Nam, S-Y. Oh, Y.J. Sun, J. Kim, W-K. Kim, S.K. Woo, W. Shin, Factors Affecting the Catalytic Epoxidation of Olefins by Iron Porphyrin Complexes and H_2O_2 in Protic Solvents, J. Org. Chem. 68 (29) (2003) 7903.
[8] S. Rayati, S. Zakavi, S.H. Motlagh, V. Noroozi, M. Razmjoo, A. Wojtczak, A. Kozakiewicz, b-Tetra-brominated meso-tetraphenylporphyrin: A conformational study and application to the Mn-porphyrin catalyzed epoxidation of olefins with tetrabutylammonium oxone, Polyhedron. 27 (11) (2008) 2285.
[9] N. Sehlotho, T. Nyokong, Catalytic activity of iron and cobalt phthalocyanine complexes towards the oxidation of cyclohexene using tert-butylhydroperoxide and chloroperoxybenzoic acid, J. Mol. Cat. A: Chem. 209 (2004) 51.
[10] K.-W. Xu, J.-Y. Ma, Q. Jiang, H.-Y. Hu, C.-C. Guo, Selective catalysis of manganese-porphyrins on aerobic oxidation of different carbon–hydrogen bonds of methyl cyclohexane, J. Mol. Catal. A: Chem. 243 (2) (2006) 194.
[11] S. Gilson de Freitas, D. Carvalho da Silva, A. Silva Guimarães, E. do Nascimento, J.S. Rebouças, M. Peres de Araujo, M.E. Moreira Dai de Carvalho, Y.M. Idemori, Cyclohexane hydroxylation by iodosylbenzene and iodobenzene diacetate catalyzed by a new β-octahalogenated Mn–porphyrin complex: The effect of meso-3-pyridyl substituents, J. Mol. Catal. A: Chem. 266 (1–2) (2007) 274.
[12] G. Labat, J. Seris, B. Meunier, Oxidative Degradation of Aromatic Pollutants by Chemical Models of Ligninase Based on Porphyrin Complexes, Angew. Chem. Int. Ed. in English 29 (12) (1990) 1471.

[13] B. Meunier, A., Robert, G. Pratviel, Metalloporphyrins in Catalytic Oxidations and Oxidative DNA Cleavage, in: K. M. Kadish, K. M. Smith, R.Guilard (Eds.), The Porphyrin Handbook, Vol. 4, Ch. 31, Academic Press, San Diego, 2000, p. 119.
[14] I. Willner, J.W. Otvos, M.J. Calvin, Preparation of an oxoporphyrinatomanganese (IV) complex, Chem. Soc. Chem. Commun. (1980) 964.
[15] J.T. Groves, M.K. Stern, Olefin epoxidation by manganese (IV) porphyrins: evidence for two reaction pathways, J. Am. Chem. Soc. 109 (1987) 3812.
[16] T. Groves, M.K. Stern, Synthesis, characterization, and reactivity of oxomanganese(IV) porphyrin complexes, J. Am. Chem. Soc. 110 (1988) 8628.
[17] J.T. Groves, J. Lee, S.S. Marla, Detection and characterization of an oxomanganese (V) porphyrin complex by rapid-mixing Stopped-flow spectrophotometry, J. Am. Chem. Soc. 119 (1997) 6269.
[18] R. Zhang, J.H. Horner, M. Newcomb, Laser Flash Photolysis Generation and Kinetic Studies of Porphyrin-Manganese-Oxo Intermediates. Rate Constants for Oxidations Effected by Porphyrin-Mn^{V}-Oxo Species and Apparent Disproportionation Equilibrium Constants for Porphyrin-Mn^{IV}-Oxo Species, J. Am. Chem. Soc. 127 (2005) 6573.
[19] C-Y. Lin, Y.O. Su, Electrocatalytic oxidation of alkenes by manganese tetrakis(N-methyl-4-pyridyl)porphine in aqueous solutions, J. Electroanal. Chem. 265 (1989) 305.
[20] F-Ch. Chen, S.-H. Cheng, Ch-H. Yu, M.-H. Liu, Y.O. Su, Electrochemical characterization and electrocatalysis of high valent manganese meso-tetrakis(N-methyl-2-pyridyl)porphyrin, J. Electroanal. Chem. 474 (1) (1999) 52–59.
[21] C-H. Yu, Y.O. Su, Electrocatalytic reduction of nitric oxide by water-soluble manganese porphyrins, J. Electroanal. Chem. 368 (1994) 323.
[22] R.D. Arasasingham, T.C. Bruice, The dynamics of the reactions of methyl diphenylhydroperoxyacetate with meso-tetrakis(2,6-dimethyl-3-sulfonatophenyl) porphinatomanganese (III) hydrate and meso-tetrakis(2,6-dichloro-3-sulfonatophenyl) porphinatomanganese (III) hydrate and imidazole complexes. Comparison of the reactions of manganese (III) and iron (III) porphyrins, J. Am. Chem. Soc. 113 (16) (1991) 6095.
[23] Electron transfer, in: K. M. Kadish, K. M. Smith, R.Guilard (Eds.), The Porphyrin Handbook, Vol. 8, Academic Press, San Diego, 2000.
[24] R.S. Czernuszewicz, Y.O. Su, M.K. Stern, K.A. Macor, D. Kim, J.T. Groves, T.G. Spiro, Oxomanganese(IV) porphyrins identified by resonance Raman and infrared spectroscopy. Weak bonds and the stability of the half-filled t2 g subshell, J. Am. Chem. Soc. 110 (13) (1988) 4158.
[25] I. M. Kolthoff, E. B. Sandell, E. J. Meehan, S. Bruckenstein Análisis Químico cuantitativo. Editorial NIGAR S.R.L. (1988).
[26] T-C. Zheng, D.E. Richardson, Homogeneous Aqueous Oxidation of Organic Molecules by Oxone® and Catalysis by a Water-Soluble Manganese Porphyrin Complex, Tetrahedron Letters 36 (6) (1995) 833.
[27] W. Zhu, W.T. Ford, Oxidation of Alkenes with Aqueous Potassium Peroxymonosulfate and No Organic Solvent, J. Org. Chem. 56 (1991) 7022.
[28] D.M. Anjo, M. Kahr, M.M. Khodabakhsh, S. Nowinski, M. Wanger, Electrochemical activation of carbon electrodes in base: minimization of dopamine adsorption and electrode capacitance, Anal. Chem. 61 (23) (1989) 2603.
[29] C. James, I. Sternberg, H.S. Stillo, R.H. Schwendeman, Spectrophotometric Analysis of Multicomponent Systems Using the Least Squares Method in Matrix Form, Anal. Chem. 32 (1) (1960) 84.
[30] S.L. Kelly, K.M. Kadish, Counterion and Solvent Effects on the Electrode Reactions of Manganese Porphyrins, Inorg. Chem. 21 (1982) 3631.
[31] N.S. Trofimova, A.Y. Safronov, O. Ikeda, Electrochemical and spectral studies on the catalytic oxidation of nitric oxide and nitrite by high-valent manganese porphyrins at an ITO electrode, Electrochim. Acta 50 (2005) 4637.
[32] A.J. Bard, L.R. Faulkner, Electrochemical Methods: Fundamentals and Applications, 2nd ed., Wiley, New York, 2001.
[33] K.M. Kadish, M. Sweetland, J.S. Cheng, Electron-transfer kinetics of chlorotetrakis(p-chlorophenyl)porphinatomanganese(III) in dimethyl sulfoxide-imidazole mixtures, Inorg. Chem. 17 (10) (1978) 2795.
[34] M. Rodriguez, A.J. Bard, Electrochemical investigation of the association of distamycin A with the manganese(III) complex of meso-tetrakis(N-methyl-4-pyridiniumyl)porphine and the interaction of this complex with DNA, Inorg. Chem. 31 (7) (1992) 1129.
[35] T.M. Cotton, S.G. Schultz, R.P. Van Duyne, Surface-enhanced resonance Raman scattering from water-soluble porphyrins adsorbed on a silver electrode, J. Am. Chem. Soc. 104 (1982) 6528.
[36] L.A. Sanchez, T.G. Spiro, Surface-enhanced Raman spectroscopy as a monitor of iron(III) protoporphyrin reduction at a silver electrode in aqueous and acetonitrile solutions: vibronic resonance enhancement amplified by surface enhancement, J. Phys. Chem. 89 (5) (1985) 763.
[37] S-P. Chen, A. Williams, D. Ejeh, P. Hambright, C.M. Hosten, Reduction of Manganese(III) Protoporphyrin IX Dimethyl Ester Studied by Electrochemistry and Surface-Enhanced Raman Scattering Spectroscopy, Langmuir 15 (1999) 3998.
[38] R.H. Wopschall, I. Shain, Effects of adsorption of electroactive species in stationary electrode polarography, Anal. Chem. 39 (13) (1967) 1514.
[39] E. Laviron, A. J. Bard Electroanalytical chemistry. Vol. 12 Marcel Dekker New York, (1982) 53.
[40] A.P. Brown, F.C. Anson, Cyclic and differential pulse voltammetric behaviour of reactants confined to the electrode surface, Anal. Chem. 49 (11) (1977) 1589.
[41] D.A. Van Galen, M. Majda, Irreversible self-assembly of monomolecular layers of a cobalt(II) hexadecyltetrapyridylporphyrin amphiphile at gold electrodes and its catalysis of oxygen reduction, Anal. Chem. 60 (15) (1988) 1549.
[42] C.H. Hamann, A. Hamnett, W. Vielstich, Electrochemistry, Wiley–VCH Weinheim, Germany, 1998.
[43] I. Tabushi, S. Kojo, Intermediacy of hematoporphyrin Mn(III) cation radical in the decay of hematoporphyrin Mn(IV) in acidic media, Tetrahedron Lett. 16 (1975) 305.
[44] A. Harriman, G. Porter, Photochemistry of manganese porphyrins. Part 2.—Photoreduction, J. Chem. Soc., Faraday Trans. 2 75 (1979) 1543.
[45] Y. Naruta, M. Sasayama, T. Sasaki, Oxygen Evolution by Oxidation of Water with Manganese Porphyrin Dimers, Angew Chem. Int. Ed. Engl. 33 (18) (1994) 1839.
[46] H. Dau, C. Limberg, T. Reier, M. Risch, S. Roggan, P. Strasser, The Mechanism of Water Oxidation: From Electrolysis via Homogeneous to Biological Catalysis, Chem. Cat. Chem. 2 (2010) 724.